p300 regulates p53-dependent apoptosis after DNA damage in colorectal cancer cells by modulation of PUMA/p21 levels

N. Gopalakrishna Iyer*†, Suet-Feung Chin*, Hilal Ozdag*, Yataro Daigo*‡, De-En Hu§, Massimiliano Cariati*, Kevin Brindle§, Samuel Aparicio*, and Carlos Caldas*¶

*Cancer Genomics Program, Department of Oncology, University of Cambridge, Hutchison/MRC Research Centre, Hills Road, Cambridge CB2 2XZ, United Kingdom; and §Department of Biochemistry, University of Cambridge, Tennis Court Road, Cambridge CB2 1GA, United Kingdom

Edited by Bert Vogelstein, The Sidney Kimmel Comprehensive Cancer Center at Johns Hopkins, Baltimore, MD, and approved March 26, 2004 (received for review February 13, 2004)

Activation of the tumor suppressor p53 by DNA damage induces either cell cycle arrest or apoptosis, but what determines the choice between cytostasis and death is not clear. In this report, we show that the E1A-binding p300 nucleoprotein is a key determinant of p53-dependent cell fate in colorectal cancer cells: absence of p300 increases apoptosis in response to DNA damage. In addition, p300-deficient (p300$^-$) cells fail to undergo G_1/S arrest after UV irradiation. These abnormalities are associated with prolongation of p53 stability, reduced p53-acetylation, blunting of MDM2 activation, failure to transactivate p21, and a disproportionate increase in PUMA levels. When xenografted, p300$^-$ cells are more sensitive to chemotherapy with doxorubicin. These results show that p300 is a key regulator of the p53 response and suggest that p300 inhibition could be used to modulate chemotherapy.

The canonical position of p53 as the guardian of the genome reflects its central role in the DNA damage response. p53 is the most frequently mutated gene in human cancers, and two mechanisms that control tumor growth are disrupted as a consequence: cell cycle arrest and apoptosis (1–5). p53 is normally activated and stabilized through a series of posttranslational modifications (predominantly phosphorylation and acetylation), in response to DNA damage (and other stress signals). Stabilized p53 protein transactivates downstream targets that mediate cell cycle arrest or apoptosis. Relative protein levels of these p53-downstream effectors determine cell fate after DNA damage. However, the mechanisms that regulate this balance remain elusive. Several factors have been implicated as modulators of the p53 response, including ARF, c-myc, and ASPP (6–8). Identifying p53 modulators and understanding the mechanisms through which they alter the p53-determined cell fate has important therapeutic implications, especially if these could be manipulated to promote apoptosis in tumors.

p300 and CBP are paralogous histone acetyltransferases that function as transcriptional regulators for several nuclear proteins (9–12). The central role of p300/CBP in cellular homeostasis is exploited by oncogenic viruses to inactivate key cellular regulators, such as p53 (13, 14). p300 and CBP participate at various stages of the p53 response (15). Both appear to be involved in controlling the stability of the p53 protein by facilitating both mdm2-dependent and -independent ubiquitination, leading to p53 degradation (16, 17). Despite this, p300 loss has not been convincingly shown to increase p53 stability in fibroblasts or in embryonic stem cells (15). In addition, p300 and CBP function as essential coactivators in p53-dependent transactivation of target genes. They promote transcription of specific p53 targets by two mechanisms. First, p300/CBP are recruited by p53 to target gene promoters where they acetylate histones (18, 19). Secondly, p53 acetylation secondary to DNA damage stabilizes the p53–DNA complex at target gene promoters. However, it is not known whether p300, CBP, or P/CAF (p300/CBP-associated factor) function as the principal p53-acetylase (20, 21). It has been suggested that p300 is more important than CBP in modulating the DNA damage response (22), but this has not been formally established.

Experiments performed on the colorectal carcinoma cell line HCT116 have been pivotal in dissecting the role of several proteins in the p53 pathway. HCT116 is a near-diploid cell line with an intact p53 response. The integrity of cell cycle checkpoints has been verified by targeting experiments, where disrupting the p53 effectors p21 and 14-3-3σ abrogates the G_1/S (p21) and G_2/M (p21 and 14-3-3σ) checkpoints (23–25). When p21 is disrupted in HCT116 cells, the p53-determined cell fate in response to DNA damage and p53 activation is altered, favoring apoptosis over arrest (26, 27). In contrast, targeting *bax* and *PUMA* disrupts the apoptotic pathway in response to p53 activation (28, 29). HCT116 is hemizygous for p300: *EP300* is expressed from a single allele, with a frameshift mutation in the last exon resulting in a protein truncated distally to the histone acetyltransferase domain (30). Despite this mutation, p300 function is intact with regard to p53 activation and acetylation in response to UV-irradiation-induced DNA damage in HCT116 (20). In addition, CBP and P/CAF are wild type in HCT116 (31). We generated three independently targeted clones null for p300 (p300$^-$) by disrupting the single expressed allele of the *EP300* gene (Fig. 5, which is published as supporting information on the PNAS web site), and two of these clones were used for subsequent experiments. Rescue clones were generated by transiently transfecting p300$^-$ cells with wild-type *EP300* cDNA. These isogenic clones were used in experiments to assess the role of p300 in the p53 response to DNA damage.

Methods

Generation of p300$^-$ and Rescue Clones. p300$^-$ cells were obtained by targeting exon 2 of the *EP300* gene (Fig. 5). Briefly, the targeting construct pIRESβ-Geo-p300KO was made by PCR amplification of the homologous arms using HCT116 genomic DNA as the template. The construct was linearized and transfected into HCT116 by using Lipofectamine PLUS (Invitrogen) according to the manufacturer's protocol. Selection was carried out by using 500 μg/ml G418, and resistant clones were screened by PCR using screening primers NeoF, 5′-GCAGCGCATCGCCTTCTATC-3′, and KO PCRScreenR, 5′-GCTCCCTCATTTGTCAAACA-3′ (data not shown). Three independently targeted clones were obtained from 217 clones screened, and two of these clones were used

This paper was submitted directly (Track II) to the PNAS office.

Abbreviation: IP, immunoprecipitation.

†Present address: Department of General Surgery, Singapore General Hospital, Outram Road, Singapore 169608.

‡Present address: Laboratory of Molecular Medicine, Human Genome Centre, Institute of Medical Science, University of Tokyo, 4-6-1 Shirokaneda, Minato Ward, Tokyo 108-8639, Japan.

¶To whom correspondence should be addressed. E-mail: cc234@cam.ac.uk.

© 2004 by The National Academy of Sciences of the USA

Downloaded at ANKARA UNIVERSITESI on December 11, 2021

in all of the experiments described below. Targeting was confirmed by Southern blotting and by immunoprecipitation (IP) Western blots showing total absence of p300 protein in p300$^-$ cells (Fig. 5). Targeted clones were expanded and frozen for subsequent experiments. Rescue clones were obtained by cotransfecting pcDEF-Flag-p300 (kind gift from M. A. Ikeda, Tokyo Medical and Dental University) expression vector with pPGK-Puro at a 10:1 ratio and selecting with 1 μg/ml Puromycin for 24 h (Fig. 5).

Tissue Culture. HCT116 (obtained from American Type Culture Collection) and its derivatives (p300$^-$ and rescue cells) were cultured in McCoy's 5A medium supplemented with 10% FCS and penicillin/streptomycin (Invitrogen). All tissue culture procedures were carried out in a Class II laminar flow hood (BioMAT 2, MAT, Derby, U.K.), and cells were grown in Sanyo CO_2 incubator MCO-17AIC at 37°C with 5% CO_2.

DNA Damage Experiments. DNA damage was carried out on subconfluent monolayers of cells as described (20). UV irradiation (10 and 25 J/m^2) was delivered by using the UV Stratalinker (Stratagene), and cells were harvested at the time points described. X-ray treatment was delivered by using the Faxitron x-ray cabinet system according to the manufacturer's protocol. Drug treatment with doxorubicin (2 μM), etoposide (34 nM), and 5-fluorouracil (12 μM) (all from Sigma and prepared according to the manufacturer's recommendations) was carried out by incubating cells with the respective concentration of the drug in fresh media for 24 h before harvesting them for apoptosis assays. All these experiments were done in triplicate for HCT116, both knockout clones and rescue cells.

Western Blots and Immunoprecipitation. Cells were harvested in protein lysis buffer [20 mM Tris·HCl, pH 7.6/150 mM NaCl/1 mM EDTA/0.5% Nonidet P-40/1 mM DTT/5 μM Trichostatin A/1 mM sodium orthovanadate/1 mM PMSF/1 mM NaF and Complete protease inhibitors (Roche Applied Science)] by passing cell suspensions through a 25-gauge needle. Western blots and immunoprecipitation were performed as described (32). All blots were performed in triplicate for HCT116, two p300$^-$, and two rescue clones. Representative examples are shown in the figures. Antibodies used include p53 (DO1) (Santa Cruz Biotechnology), p53 (Ab2), phospho-p53 (ser15) (Ab-3), Ac-p53 (K382) (Ab1), mdm2 (Ab1), p21/WAF1 (Ab1), Noxa (Ab1) (Oncogene), bax (B3428) (Sigma), and Puma (kind gift from B. Vogelstein).

Apoptosis Assays. To determine apoptotic fractions, cells were harvested before and 24 h after various forms of DNA damage. Cells were then analyzed by using the TACS Annexin V-FITC (R & D Systems) apoptosis detection kit according to the manufacturer's protocol. The DNA damage experiments were done in triplicate for each cell line (HCT116, two p300$^-$ clones, and rescue cells). Apoptotic fractions were determined by flow cytometry, where cells positive for Annexin V staining but not propidium iodide were counted. Although this method tends to underestimate the apoptotic cell fraction, it excludes necrotic cells. Apoptosis was confirmed by terminal deoxynucleotidyltransferase-mediated dUTP nick end labeling (TUNEL) staining with the Fluorometric TUNEL system (Promega) according to the manufacturer's protocol and immunoblotting with cleaved caspase-3 antibodies (Cell Signaling Technology, Beverly, MA).

cDNA Synthesis and Real-Time PCR. HCT116, p300$^-$ (two clones), and rescue cells were treated with 25 J/m^2 UV-C irradiation as described and harvested at 0, 3, 6, 12, and 24 h after treatment. RNA was isolated from these cells by using TRIzol reagent (Invitrogen) according to the manufacturer's protocol. cDNA was synthesized by reverse transcription of 2 μg of total RNA with random hexamers. Real-time PCR was carried out by using SYBR Green PCR Master Mix on an ABI 7900 Sequence Detection System (Applied Biosystems). The specificity of the PCR products was confirmed by melting curve analysis with ABI SDS 2.0 software. Relative expression levels were calculated based on the difference in C_T values between the test samples (treated and untreated HCT116, p300$^-$, and rescue cells) and control (untreated HCT116 cells). This was normalized with expression levels of GAPDH by using the equation $E_{\text{target}}(C_{\text{Ttest}}{}^{\text{target}} - C_{\text{Tcontrol}}{}^{\text{target}})/E_{\text{ref}}$ $(C_{\text{Ttest}}{}^{\text{ref}} - C_{\text{Tcontrol}}{}^{\text{ref}})$ as described (33). The experiment was carried out in triplicate on all cell types. The mean expression levels obtained were plotted against time after UV treatment. Primers used in these analyses were as follows: GAPDH F, 5′-TTTAACTCTGGTAAAGTGGA-3′, and GAPDH R, 5′-GAATCATATTGGAACATGTA-3′; MDM2 F, 5′-ATCTTGGCCAGTATATTATG-3′, and MDM2 R, 5′-GTTCCTGTAGATCATGGTAT-3′; p21 F, 5′-GGACCTGGAGACTCTCA-3′, and p21 R, 5′-CCTCTTGGAGAAGATCAG-3′; PUMA F, 5′-GACCTCAACGCACAGTA-3′, and PUMA R, 5′-CTAATTGGGCTCCATCT-3′; NOXA F, 5′-ACTGTTCGTGTTCAGCTC-3′, and NOXA R, 5′-GTAGCACACTCGACTTCC-3′.

Cell Line Xenograft Studies. HCT116 and two p300$^-$ clones were implanted s.c. in SCID mice (1×10^6 cells). Xenografts experiments were done by implanting 12 mice with the respective cells (6 treated and 6 untreated controls). Xenografted tumors were measured by using calipers (major and minor axis) every 2 days, once they were palpable (10–15 days after implantation). Tumor volumes were calculated by using the equation length $\times$ width^2 $\times$ 0.5. Doxorubicin treatment was delivered as a single i.v. bolus treatment (at a dose of 8 mg/kg of body weight by tail vein injection) once tumor volumes reached $\approx$400 mm^3. Relative tumor volumes were plotted by dividing average tumor volume for each data point by the average starting tumor volume.

Results

p300 Is Required for p53 Acetylation After UV-Induced DNA Damage in HCT116 Cells. In response to UV-induced DNA damage, p53 is acetylated at lysine residues 373 and 382 by p300/CBP (20). The acetylation status at p53-Lys-382 in HCT116, p300$^-$ (two clones), and rescue cells was determined by IP Western blots (Fig. 1*A*). After UV irradiation, p53 acetylation was present in almost undetectable levels in p300$^-$ cells when compared to HCT116. p53 acetylation was restored to normal levels in rescue cells. These experiments showed that in a cell line expressing wild-type CBP and P/CAF, p300 is both necessary and sufficient for the acetylation of lysine 382 in the p53 protein after UV-induced DNA damage.

p53 Stability Is Increased in Response to UV-Induced DNA Damage in p300$^-$ Cells. After UV irradiation, p53 protein levels increased in both HCT116 and p300$^-$ cells, reaching maximal levels 12–24 h after damage (Fig. 1*B*), indicating that p300 loss and reduced p53 acetylation had no effect on p53 induction. However, p53 protein levels remained elevated in p300$^-$ cells for up to 48 h after damage, showing that p53 stability is increased. p53 activation is usually accompanied by phosphorylation at Ser-15. Phospho-p53 levels were similarly sustained in p300$^-$ cells after damage (data not shown). In rescue cells, p53 and phospho-p53 were restored to levels comparable to those seen in HCT116. Western blots (Fig. 1*B*) also showed that MDM2 activation was blunted in p300$^-$ cells, with protein levels not sustained after UV treatment for as long as in HCT116 cells. Real-time PCR also showed reduced mdm2 transcription in p300$^-$ cells (Fig. 1*C*). In rescue cells, mdm2 transcription and protein expression levels were restored (Fig. 1 *B* and *C*). These data show that, as a direct result of p300 inactivation, p53 stability is increased after DNA damage, in association with reduced mdm2 activation.

Downloaded at ANKARA UNIVERSITESI on December 11, 2021

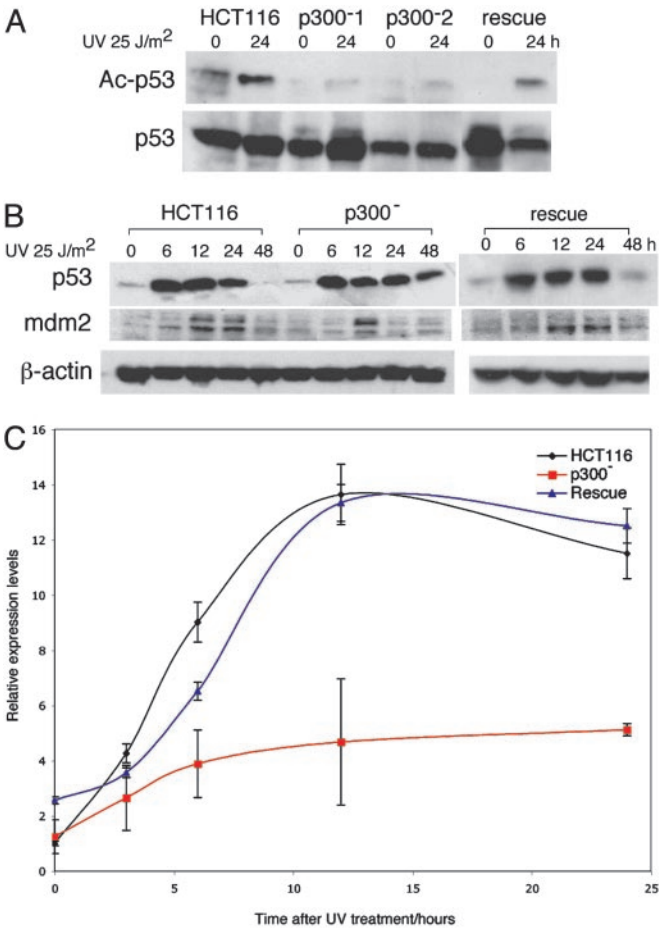

Fig. 1. p53 acetylation and stability after UV irradiation. (*A*) IP Western blots of p53 acetylation in HCT116, p300$^-$, and rescue cells 24 h after UV irradiation. IP was done by using p53-DO1 antibody and blotted by using Ac-Lys-382 and p53 (Ab2) antibodies. (*B*) Western blot showing p53 and mdm2 levels in HCT116, p300$^-$, and rescue cells after UV irradiation with 25 J/m^2 UV-C at the time points indicated. (*C*) Graph of relative expression levels determined by RT-PCR of MDM2 in HCT116, p300$^-$, and rescue cells after UV irradiation. Relative expression levels represent the mean of triplicate experiments performed for each of the cell types, with error bars representing two standard deviations.

Activation of p53 Target Genes After DNA Damage Is Altered in p300$^-$ Cells. To analyze the downstream effect of reduced acetylation and increased stability of p53 the protein, levels of several p53 targets that mediate cell cycle arrest (p21) and apoptosis (PUMA, Noxa, and Bax) were determined at baseline and after UV irradiation (Fig. 2*A*). Despite higher baseline levels in p300$^-$ cells there was no increase in p21 protein after DNA damage. This pattern differed significantly in HCT116 cells where a rise in p21 levels was seen, as previously reported. The higher baseline p21 levels seen in p300$^-$ asynchronous cultures were due to the presence of a noncycling cell population (in G_0) (data not shown). In sharp contrast, increased PUMA levels after DNA damage were sustained for a longer period in p300$^-$ cells compared to HCT116. In rescue cells, levels of p21 and PUMA were comparable to HCT116. p300 absence appeared to have no effect on NOXA and bax, after UV-induced damage, with both proteins having similar profiles in HCT116 and p300$^-$ cells.

p21 and PUMA are known direct transcriptional targets of p53, and levels of each transcript were quantified by RT-PCR (Fig. 2*B*). The aim was to determine whether increased protein levels could be explained, at least in part, by increased transcription. In HCT116 cells, p21 expression increased after UV-mediated DNA damage. In p300$^-$ cells, whereas baseline levels of p21 expression were slightly higher that in HCT116 (as seen in Western blots), transcription did not increase after UV irradiation. In rescue cells, p21 expression was restored to levels seen in HCT116. The results for PUMA transcription were markedly different: PUMA expression increased to much higher levels in p300$^-$ cells compared to HCT116. In rescue cells, PUMA expression was restored to similar levels to those seen in HCT116. Importantly the ratio of PUMA/p21 expression was significantly higher in p300$^-$ clones compared with HCT116 and rescue cells. These results show that in response to DNA damage, the loss of p300 results in blunted p21 activation coupled with a disproportionate increase in PUMA activation.

p300$^-$ Cells Fail to Arrest and Undergo Apoptosis After UV-Induced DNA Damage. Under routine culture conditions we noted that p300$^-$ cells compared with HCT116 have a proliferation defect associated with increased doubling times (28 ± 2 h versus 18.8 ± 0.6 h) but no increase in apoptosis. After UV-induced DNA damage it is known that HCT116 cells normally undergo cell cycle arrest. To determine the effects of p300 disruption in cell cycle progression after damage, UV-irradiated cells were pulsed with BrdUrd and analyzed by using flow cytometry (Fig. 3*A*). p300$^-$ cells failed to undergo cell cycle arrest at the G_1/S checkpoint: 25% of p300$^-$ cells were still incorporating BrdUrd 24 h after DNA damage compared to a negligible proportion of HCT116 cells. In contrast, a significantly higher proportion of p300$^-$ cells underwent apoptosis in response to UV irradiation. The increase in apoptosis was quantified by Annexin V staining/flow cytometry (Fig. 3*B*) and confirmed by terminal deoxynucleotidyltransferase-mediated dUTP nick end labeling (TUNEL) staining (data not shown) and cleaved caspase-3 Western blots (Fig. 3*C*). The results of these experiments show that loss of p300 in HCT116 significantly alters the response to UV-induced DNA damage, favoring apoptosis over arrest. The difference in response was a direct effect of p300 loss, because in rescue clones the balance between arrest and apoptosis was restored to the levels seen in HCT116 (Fig. 3*B* and data not shown).

p300 Absence Increases Apoptosis in Response to Different Forms of DNA Damage. HCT116, p300$^-$, and rescue cells were treated with DNA-damaging agents besides UV irradiation: etoposide, doxorubicin, 5-FU, and x-ray irradiation. After DNA damage the fraction of cells undergoing apoptosis was quantified by using Annexin V staining and flow cytometry (Fig. 3*B*). p300$^-$ cells, compared to HCT116, were found to be more sensitive to etoposide, doxorubicin, and 5-FU, with a significantly higher proportion undergoing apoptosis 24 h after treatment. Increased apoptosis was confirmed by TUNEL assays and cleaved caspase-3. This increased sensitivity to DNA damage was reversed in rescue cells. Both HCT116 and p300$^-$ cells displayed minimal apoptosis after DNA damage with x-ray irradiation. These results show that in HCT116 cells the specific loss of p300 is sufficient to promote sensitivity *in vitro* to different forms of DNA damage.

p53 Response of p300$^-$ Cells to Doxorubicin Is Similar to That Seen with UV Irradiation. Despite the different types of DNA damage induced (with doxorubicin, double-strand breaks, and with UV irradiation, pyrimidine dimers), p300$^-$ cells responded to doxorubicin treatment by undergoing apoptosis similarly to what was seen after UV treatment. We tested whether this was also mediated by an altered p53 response. IP Western blots showed that p53-acetylation is reduced in p300$^-$ cells after doxorubicin treatment, compared to HCT116 and rescue cells (Fig. 4*A*). Western blots (Fig. 4*B*) showed prolonged p53 protein stability, blunted p21 activation, and a disproportionate increase in PUMA levels in p300$^-$ cells. All of these abnormalities were reversed in rescue cells. These results confirm that absence of p300 results in abnormalities in the p53

Downloaded at ANKARA UNIVERSITESI on December 11, 2021

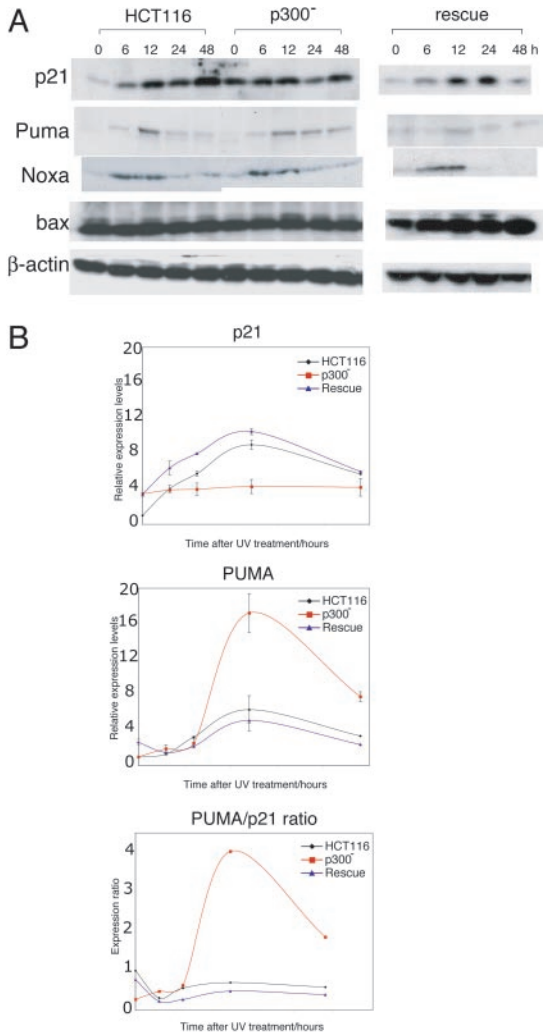

Fig. 2. p53 target gene activation after UV irradiation. (*A*) Western blots showing levels of p21, PUMA, NOXA, and bax in HCT116, p300$^-$, and rescue cells after UV irradiation (25 J/m^2 UV-C) at various time points as indicated. (*B*) Graph of relative expression levels determined by RT-PCR of p21, PUMA, and PUMA/p21 expression ratio in HCT116, p300$^-$, and rescue cells after UV irradiation. Relative expression levels represent the mean of triplicate experiments performed for each of the cell types, with error bars representing two standard deviations.

response after doxorubicin similar to those seen with UV-mediated DNA damage.

p300$^-$ Xenografts Are More Sensitive to Doxorubicin Treatment. To examine whether the increased apoptosis induced by doxorubicin in p300$^-$ cells translated to differences in drug sensitivity *in vivo*, HCT116 and p300$^-$ cells were implanted in SCID mice to generate tumors (Fig. 4*C*). When tumor volumes reached ≈400 mm^3, mice were treated with a single dose of i.v. doxorubicin (8 mg/kg body weight). HCT116 xenografts showed no response to the drug. In contrast, tumors derived from p300$^-$ cells responded with an immediate cessation of tumor growth. This difference in response was statistically significant and showed that p300 disruption sensitized resistant tumors with wild-type p53 to chemotherapy.

Discussion

The key question in the p53 response to DNA damage remains: What determines why some cells die whereas others arrest? Different models of regulation of the p53 response have emerged (34).

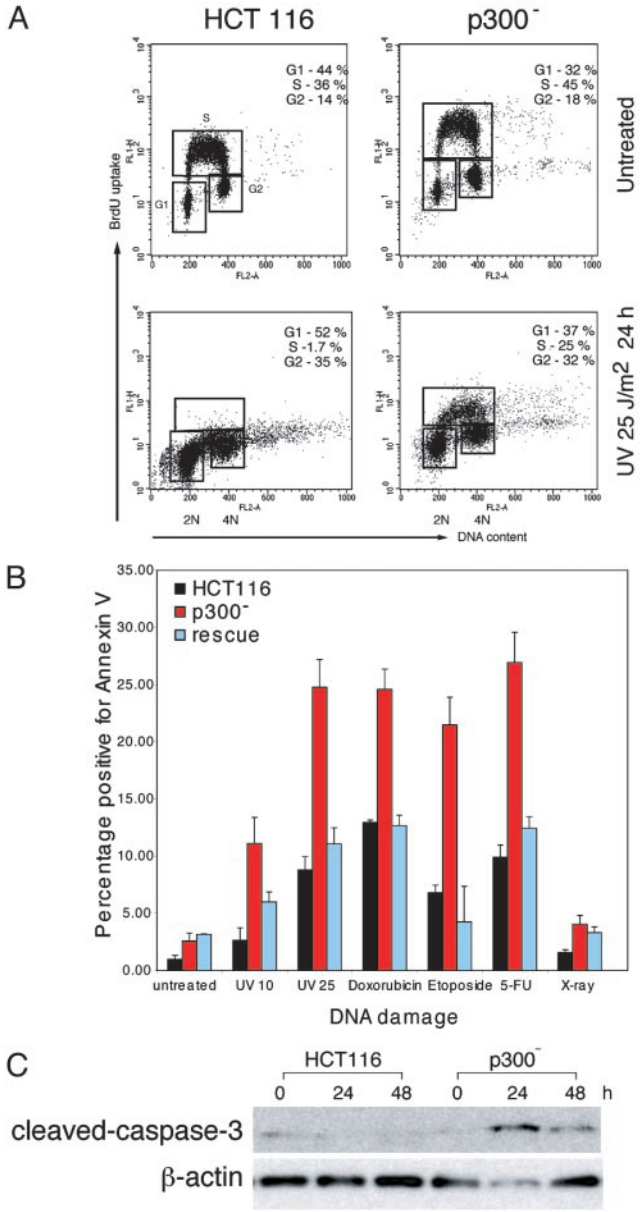

Fig. 3. Response of HCT116, p300$^-$, and rescue cells to DNA damage. (*A*) Flow cytometry analysis of BrdUrd incorporation 24 h after treatment with UV 25 J/m^2. Cell cycle fractions are indicated. (*B*) Graph showing apoptotic fractions (i.e., cells positive for Annexin V binding) in cells treated with various forms of DNA damage as indicated: untreated, 10 J/m^2 UV, 25 J/m^2 UV, 2 μM doxorubicin, 34 nM etoposide, 15 μg/ml 5-fluorouracil (5-FU), and 10 Gy of x-ray irradiation. (*C*) Western blot showing levels of cleaved caspase-3 in HCT116 and p300$^-$ cells, after irradiation with 10 J/m^2 UV-C.

One model says the p53 activity remains constant, and the outcome is determined by the presence or absence of apoptotic signals cooperating with p53 to reach a death threshold. A second model proposes the response is determined by the regulation of p53's DNA binding and transcriptional activity. A third model suggests that the key event is blocking the expression of p53-induced inhibitors of cell death, an example being c-myc-mediated suppression of p21 (6). In our data, c-myc protein levels were similar in HCT116 and p300$^-$ cells both at baseline and after DNA damage (data not shown). Experiments performed by using the colorectal cancer cell line HCT116 have been instrumental in providing support for one or more of these models. We used HCT116 cells to

Downloaded at ANKARA UNIVERSITESI on December 11, 2021

interrogate the p53 response in the presence and absence of p300, a known regulator of p53 posttranslational modification and a p53 coactivator, and based on the observations reported here, we propose a model.

The first result was that p300 disruption in HCT116, a cell line with wild-type CBP and pCAF, results in impaired p53 acetylation in response to UV irradiation and doxorubicin. This finding shows that in these cells p300, and not CBP or pCAF, is the main p53 acetylase in the DNA damage response. Because p53 acetylation is significantly impaired, this provided us with an experimental system to determine whether such acetylation is required to mount a proper p53-dependent DNA damage response, an important unanswered question (15).

The second (perhaps unexpected) result was that p300 disruption is associated with increased p53 stability after UV irradiation and doxorubicin. Several mechanisms could account for this increased p53 stability. First, mdm2 activation after DNA damage is reduced in p300$^-$ cells (Fig. 1 *B* and *C*). In rescue clones, mdm2 activation is restored to levels similar to those seen in HCT116. These results show that p300 is necessary for the transactivation of mdm2 in the DNA damage response. Because mdm2 functions to target p53 for degradation, a blunted mdm2 response would result in sustained p53 levels. In previous studies, p300 deficiency induced by ribozymes was shown to markedly reduce p53-mediated transactivation of the *MDM2* promoter, resulting in defective MDM2 induction in response to DNA damage (22). Others have also reported that p300 plays a role in p53-mediated induction of MDM2 (35). These published accounts, together with the data reported here, show that p300 is essential for MDM2 activation. Second, MDM2-mediated p53 ubiquitination and degradation depends on p300 and the formation of a p53–MDM2–p300 ternary complex (16, 17). Hence, loss of p300 itself contributes to decreased mdm2-dependent p53 degradation. Third, p300 could directly contribute to p53's degradation, and its absence would result in increased p53 stability. Indeed, purified p300 exhibits ubiquitin ligase activity responsible for *in vivo* polyubiquitination of p53 (17). Finally, p53 acetylation could be necessary for MDM2-dependent degradation. Data have been published suggesting that a lack of p53 acetylation interferes with MDM2-dependent ubiquitination and degradation (36).

The third and most significant result was the altered DNA damage response in p300$^-$ cells. After DNA damage and stabilization of p53, it is not entirely clear how a cell chooses between apoptosis and p21-dependent cell cycle arrest (37). Colorectal carcinoma cell lines respond to exogenous p53 expression either by cell cycle arrest (A-type cell lines) or apoptosis (D-type lines) (27). HCT116 is an A-type cell line: p53 overexpression results in cell cycle arrest. Targeted disruption of p21 in HCT116 abrogates cell cycle arrest and increases apoptosis (23, 26). However, disruption of p21 in HCT116 cells promotes apoptosis only when PUMA is intact (29). These experiments suggest that the balance between PUMA and p21 is pivotal in determining the responses to p53 activation. Nevertheless, they fail to unravel the mechanism by which the balance is regulated. Our results show that p300 disruption converts an "A-type" cell line into a "D-type" cell line, in association with altered p53 modulation such that p21 activation is blunted and PUMA activation is increased. The role for p300 in p53-dependent activation of p21 has previously been examined: p53-acetylation-dependent recruitment of coactivators/HATs was shown to be crucial (18). In addition, p300-dependent p21 coactivation is an important component of p300-dependent cell cycle arrest (38). Therefore, it was not surprising to find that loss of p300 results in failure to activate p21 transcription. More unexpected was the marked increase in PUMA transcription. PUMA was first identified as a proapoptotic p53 transcriptional target gene (39, 40). The results reported here suggest that loss of p300 may actually increase p53-dependent activation of PUMA, although the mechanism for this response is unclear. We did notice that in rescue cells, PUMA expression was not completely restored to levels seen in parental HCT116 (Figs. 2*A* and 4*B*), suggesting that p300 overexpression may indeed suppress PUMA activation. Nevertheless, because these results were from transient transfection studies, which are not necessarily physiological, we would interpret this observation with caution.

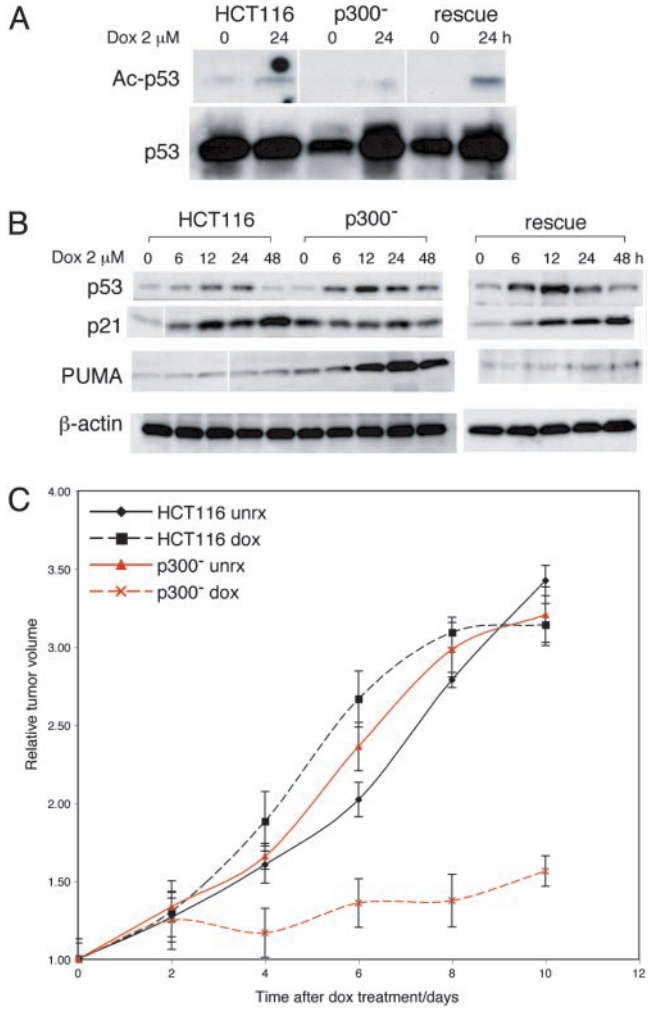

Fig. 4. Response of HCT116 and p300$^-$ cells and xenografts to doxorubicin treatment. (*A*) IP Western blots of p53 acetylation in HCT116, p300$^-$, and rescue cells 24 h after treatment with 2 μM doxorubicin. IP was done by using p53-DO1 antibody and blotted by using Ac-Lys-382 and p53 (Ab2) antibodies. (*B*) Western blots showing levels of p53, p21, and PUMA in HCT116, p300$^-$, and rescue cells after doxorubicin treatment (2 μM) at various time points as indicated. (*C*) Graph of relative tumor volumes in HCT116 and p300$^-$ xenografts after doxorubicin treatment and untreated controls. The plotted values are average volumes from cohorts of treated (six mice) and untreated controls (six mice), with error bars indicating two standard deviations.

The increased apoptosis in the absence of p300 was not restricted to one form of DNA damage, and extended to several chemotherapy agents (Fig. 3*B*). It has been suggested that apoptosis is a better assay to predict *in vivo* response to cytotoxic therapy than the clonogenic survival assay (41, 42). This prompted us to test whether p300$^-$ cells would be more sensitive to chemotherapy when using an *in vivo* model. Experiments with xenografts derived from HCT116 and p300$^-$ cells provided compelling evidence that p300 loss increases sensitivity of tumors to doxorubicin treatment. This finding suggests that p300 inhibition could be used to modulate chemotherapy in colorectal tumors with wild-type p53. This hy-

Downloaded at ANKARA UNIVERSITESI on December 11, 2021

pothesis can now be tested, both *in vitro*, taking advantage of the isogenic human cancer cells described here, an approach of demonstrated value (43), and *in vivo*, by using the xenograft model. Another potential clinical application of these findings is that the analysis of expression levels of p300 in colorectal tumors with wild-type p53 could be used to predict response to chemotherapy.

The distinction between cell cycle arrest and apoptosis induction may depend on differences in the interaction of p53 with coactivators or on changes in the activity of other pathways in the cell, as has been suggested (44). Based on our results we propose a model of regulation where levels of p300 are critical in determining the p53 response after DNA damage. When p300 levels are not limiting, p53 activation is transient and results in the transactivation of p21, with minimal activation of proapoptotic pathways. If p300 levels are low or absent, the combination of increased p53 stability [which *per se* could result in increased apoptosis (35)], reduced transcription of p21, and increased PUMA activation favors apoptosis over arrest.

We thank M. A. Ikeda and B. Vogelstein for kindly providing reagents, and Sarah Hyland and Lucy Jackson for technical assistance. N.G.I. was the recipient of a National Medical Research Council (Singapore) Medical Research Fellowship. This work was supported by Cancer Research UK.

1. Prives, C. & Hall, P. A. (1999) *J. Pathol.* **187,** 112–126.
2. Ko, L. J. & Prives, C. (1996) *Genes Dev.* **10,** 1054–1072.
3. Sherr, C. J. & McCormick, F. (2002) *Cancer Cell* **2,** 103–112.
4. Sherr, C. J. (1998) *Genes Dev.* **12,** 2984–2991.
5. Fei, P. & El-Deiry, W. S. (2003) *Oncogene* **22,** 5774–5783.
6. Seoane, J., Le, H. V. & Massague, J. (2002) *Nature* **419,** 729–734.
7. Hemmati, P. G., Gillissen, B., von Haefen, C., Wendt, J., Starck, L., Guner, D., Dorken, B. & Daniel, P. T. (2002) *Oncogene* **21,** 3149–3161.
8. Slee, E. A. & Lu, X. (2003) *Toxicol. Lett.* **139,** 81–87.
9. Giles, R. H., Peters, D. J. & Breuning, M. H. (1998) *Trends Genet.* **14,** 178–183.
10. Giordano, A. & Avantaggiati, M. L. (1999) *J. Cell Physiol.* **181,** 218–230.
11. Goodman, R. H. & Smolik, S. (2000) *Genes Dev.* **14,** 1553–1577.
12. Chan, H. M. & La Thangue, N. B. (2001) *J. Cell Sci.* **114,** 2363–2373.
13. Somasundaram, K. & El-Deiry, W. S. (1997) *Oncogene* **14,** 1047–1057.
14. Patel, D., Huang, S. M., Baglia, L. A. & McCance, D. J. (1999) *EMBO J.* **18,** 5061–5072.
15. Grossman, S. R. (2001) *Eur. J. Biochem.* **268,** 2773–2778.
16. Grossman, S. R., Perez, M., Kung, A. L., Joseph, M., Mansur, C., Xiao, Z. X., Kumar, S., Howley, P. M. & Livingston, D. M. (1998) *Mol. Cell* **2,** 405–415.
17. Grossman, S. R., Deato, M. E., Brignone, C., Chan, H. M., Kung, A. L., Tagami, H., Nakatani, Y. & Livingston, D. M. (2003) *Science* **300,** 342–344.
18. Barlev, N. A., Liu, L., Chehab, N. H., Mansfield, K., Harris, K. G., Halazonetis, T. D. & Berger, S. L. (2001) *Mol. Cell* **8,** 1243–1254.
19. Espinosa, J. M. & Emerson, B. M. (2001) *Mol. Cell* **8,** 57–69.
20. Sakaguchi, K., Herrera, J. E., Saito, S., Miki, T., Bustin, M., Vassilev, A., Anderson, C. W. & Appella, E. (1998) *Genes Dev.* **12,** 2831–2841.
21. Dornan, D., Shimizu, H., Perkins, N. D. & Hupp, T. R. (2003) *J. Biol. Chem.* **278,** 13431–13441.
22. Yuan, Z. M., Huang, Y., Ishiko, T., Nakada, S., Utsugisawa, T., Shioya, H., Utsugisawa, Y., Yokoyama, K., Weichselbaum, R., Shi, Y. & Kufe, D. (1999) *J. Biol. Chem.* **274,** 1883–1886.
23. Waldman, T., Kinzler, K. W. & Vogelstein, B. (1995) *Cancer Res.* **55,** 5187–5190.
24. Bunz, F., Dutriaux, A., Lengauer, C., Waldman, T., Zhou, S., Brown, J. P., Sedivy, J. M., Kinzler, K. W. & Vogelstein, B. (1998) *Science* **282,** 1497–1501.
25. Chan, T. A., Hermeking, H., Lengauer, C., Kinzler, K. W. & Vogelstein, B. (1999) *Nature* **401,** 616–620.
26. Javelaud, D. & Besancon, F. (2002) *J. Biol. Chem.* **277,** 37949–37954.
27. Polyak, K., Waldman, T., He, T. C., Kinzler, K. W. & Vogelstein, B. (1996) *Genes Dev.* **10,** 1945–1952.
28. Zhang, L., Yu, J., Park, B. H., Kinzler, K. W. & Vogelstein, B. (2000) *Science* **290,** 989–992.
29. Yu, J., Wang, Z., Kinzler, K. W., Vogelstein, B. & Zhang, L. (2003) *Proc. Natl. Acad. Sci. USA* **100,** 1931–1936.
30. Gayther, S. A., Batley, S. J., Linger, L., Bannister, A., Thorpe, K., Chin, S. F., Daigo, Y., Russell, P., Wilson, A., Sowter, H. M., *et al.* (2000) *Nat. Genet.* **24,** 300–303.
31. Ozdag, H., Batley, S. J., Forsti, A., Iyer, N. G., Daigo, Y., Boutell, J., Arends, M. J., Ponder, B. A., Kouzarides, T. & Caldas, C. (2002) *Br. J. Cancer* **87,** 1162–1165.
32. Langley, E., Pearson, M., Faretta, M., Bauer, U. M., Frye, R. A., Minucci, S., Pelicci, P. G. & Kouzarides, T. (2002) *EMBO J.* **21,** 2383–2396.
33. Pfaffl, M. W. (2001) *Nucleic Acids Res.* **29,** e45.
34. Vousden, K. H. (2002) *Cancer Cell* **2,** 351–352.
35. Thomas, A. & White, E. (1998) *Genes Dev.* **12,** 1975–1985.
36. Nakamura, S., Roth, J. A. & Mukhopadhyay, T. (2000) *Mol. Cell. Biol.* **20,** 9391–9398.
37. Gartel, A. L. & Tyner, A. L. (2002) *Mol. Cancer Ther.* **1,** 639–649.
38. Lee, C. W., Sorensen, T. S., Shikama, N. & La Thangue, N. B. (1998) *Oncogene* **16,** 2695–2710.
39. Yu, J., Zhang, L., Hwang, P. M., Kinzler, K. W. & Vogelstein, B. (2001) *Mol. Cell* **7,** 673–682.
40. Nakano, K. & Vousden, K. H. (2001) *Mol. Cell* **7,** 683–694.
41. Lamb, J. R. & Friend, S. H. (1997) *Nat. Med.* **3,** 962–963.
42. Waldman, T., Zhang, Y., Dillehay, L., Yu, J., Kinzler, K., Vogelstein, B. & Williams, J. (1997) *Nat. Med.* **3,** 1034–1036.
43. Torrance, C. J., Agrawal, V., Vogelstein, B. & Kinzler, K. W. (2001) *Nat. Biotechnol.* **19,** 940–945.
44. Kaeser, M. D. & Iggo, R. D. (2002) *Proc. Natl. Acad. Sci. USA* **99,** 95–100.

Downloaded at ANKARA UNIVERSITESI on December 11, 2021